

Antiferromagnetic sawtooth chain with spin- $\frac{1}{2}$ and spin-1 sites

V. Ravi Chandra,¹ Diptiman Sen,¹ N. B. Ivanov,^{2,*} and J. Richter²

¹Centre for Theoretical Studies, Indian Institute of Science, Bangalore 560012, India

²Institut für Theoretische Physik, Universität Magdeburg, PF 4120, D-39016 Magdeburg, Germany

We study the low-energy properties of a sawtooth chain with spin-1's at the bases of the triangles and spin- $\frac{1}{2}$'s at the vertices of the triangles. The spins have Heisenberg antiferromagnetic interactions between nearest neighbors, with a coupling J_2 between a spin-1 and a spin- $\frac{1}{2}$, and a coupling $J_1=1$ between two spin-1's. Analysis of the exact diagonalization data for periodic chains containing up to $N=12$ unit cells shows that the ground state is a singlet for exchange couplings up to approximately $J_2=3.8$, whereas for larger J_2 the system exhibits a ferrimagnetic ground state characterized by a net ferromagnetic moment per unit cell of $1/2$. In the region of small interactions J_2 , the mixed spin sawtooth chain maps on to an effective isotropic spin model representing two weakly interacting and frustrated spin- $\frac{1}{2}$ Heisenberg chains composed of spin- $\frac{1}{2}$ sites at odd and even vertices, respectively. Finally, we study the phenomenon of a macroscopic magnetization jump which occurs if a magnetic field is applied with a value close to the saturation field for $J_2=2$.

I. INTRODUCTION

There has been a great deal of interest in recent years in one-dimensional quantum spin systems with frustration.¹ The most common examples of such systems are those in which triangles of Heisenberg spins interact antiferromagnetically with each other. Some of the systems which have been studied analytically or numerically so far are the sawtooth spin- $\frac{1}{2}$ chain,²⁻⁴ a chain of spin- $\frac{1}{2}$ triangles,⁵ frustrated mixed spin ferrimagnetic chains,⁶ and the spin- $\frac{1}{2}$ kagomé strip.^{7,8} There is also a recent study of a spin- $\frac{1}{2}$ -spin-1 system on a diamond lattice which exhibits a number of phases as a function of the various couplings.⁹ Examples of quasi-one-dimensional frustrated spin systems which have been studied experimentally include a sawtooth spin- $\frac{1}{2}$ system,³ a zigzag spin- $\frac{1}{2}$ chain,¹⁰ and a mixed spin- $\frac{1}{2}$ -spin-1-system.¹¹

Classically, i.e., in the limit in which the magnitudes of the spins $S_i \rightarrow \infty$, some of these frustrated systems have an enormous ground-state degeneracy arising from local rotational degrees of freedom which cost no energy. Quantum mechanically, this degeneracy is often lifted due to tunneling between different classical ground states. However, one might still expect a remnant of the classical degeneracy in the form of a large number of low-energy excitations in the quantum system.

Recently, the ground state of the spin- $\frac{1}{2}$ sawtooth chain has been numerically studied as a function of the ratio J_2/J_1 , where J_1 is the coupling between pairs of spins at the bases of the triangles, and J_2 is the coupling between a spin at the base and a spin at the vertex of a triangle.⁴ The system was found to be gapless for $J_2/J_1 > 2.052$ and for $J_2/J_1 < 0.65$. The low-energy excitations have the same dispersion for singlets and triplets. For $J_2/J_1 = 1$, the system has some special properties. The ground state of an open chain has an exact degeneracy which increases linearly with the number of triangles.^{2,3} This degeneracy arises from the existence of localized spin- $\frac{1}{2}$ kinks which do not cost any energy regardless of their position in the chain. There are also spin- $\frac{1}{2}$ antikinks

which cost a finite energy. The lowest excitation in a chain with periodic boundary conditions is given by a kink-antikink pair which has a dispersionless gap; the pair may be either a singlet or triplet.

As the couplings between the different spins are varied, one-dimensional spin systems may undergo phase transitions at zero temperature, such as from a gapless phase with long-range order to a gapped phase with short-range order.¹² The different phases can often be distinguished from each other by looking at properties such as the magnetic susceptibility at low temperatures.

In this paper, we will carry out analytical and numerical studies of a mixed spin Heisenberg antiferromagnet on the sawtooth lattice shown in Fig. 1. The arrows and angles (θ) shown in that figure refer to a canted state which will be discussed later. The sites at the vertices of the triangles have spin S_2 , and they are labeled $1, 2, \dots, N$. The sites at the bases of the triangles have spin S_1 , and they are labeled $N+1, N+2, \dots, 2N$. The number of triangles is therefore N . The Hamiltonian governing the system is

$$H = J_1 \sum_{i=N+1}^{2N} \vec{S}_i \cdot \vec{S}_{i+1} + J_2 \sum_{i=1}^N \vec{S}_i \cdot (\vec{S}_{i+N} + \vec{S}_{i+N+1}), \quad (1)$$

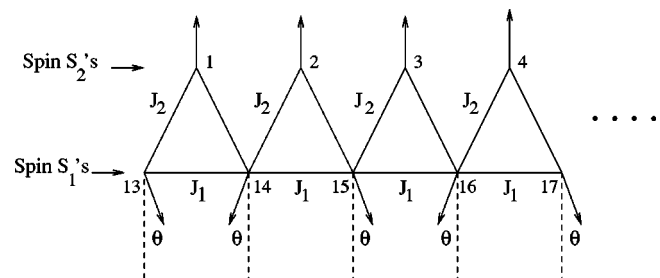


FIG. 1. Picture of the first four triangles of a sawtooth chain with $N=12$ indicating the site labels for the spin- S_2 's at the vertices and the spin- S_1 's at the bases of the triangles, and the couplings J_1 and J_2 . For the numerical studies, we take $S_1=1$ and $S_2=\frac{1}{2}$. The arrows and angles (θ) indicate a canted state in which all the spin- S_2 's are aligned with each other.

where the couplings J_1 and J_2 are positive. It is convenient to set $J_1=1$ and to consider the properties of the system as a function of J_2 . We will impose periodic boundary conditions at the ends of the chain, so that the momentum is a good quantum number. We will set Planck's constant $\hbar=1$, and the nearest-neighbor lattice spacings equal to 1.

The plan of our paper is as follows. In Sec. II, we will develop the spin-wave theory (SWT) for this system,¹³ taking the values of the spin S_1 at the bases and the spin S_2 at the vertices of the triangles to be very large, and $S_1>S_2$. If $J_2>2S_1/S_2$, we find that the system is a ferrimagnet, with a magnetization per unit cell of S_1-S_2 . If $J_2<2S_1/S_2$, we find that there is an infinite number of classical ground states as mentioned above. For reasons explained below, we will consider the classical ground states which are coplanar; the number of even this restricted set of states grows exponentially with N . We perform a linear SWT about these coplanar states, and find that the spin-wave zero point energy does not break the classical degeneracy. Further, one of the spin-wave modes turns out to have zero energy for all momenta. We will also see that SWT picks out two other values of J_2 (i.e., $J_2=1$ and 2), as being special.

In Sec. III, we use the Lanczos algorithm to perform an exact diagonalization (ED) of finite systems to study the low-energy excitations and two-spin correlations in the ground state as a function of J_2 for $S_1=1$ and $S_2=1/2$. We find that the system is a ferrimagnet for $J_2\geq 3.8$ with a magnetization per unit cell of $1/2$. We see that the transition to a collinear ferrimagnetic state takes place at a smaller value of J_2 in the quantum case than in the classical case where the transition occurs at $J_2=4$. This effect has already been seen for other systems exhibiting transitions between collinear and noncollinear states (see, for example, Ref. 6), and it indicates a favoring of the collinear state by quantum fluctuations. There seems to be a first-order transition at $J_2\approx 3.8$ with the total spin of the ground state changing rather abruptly at that value. For $J_2\leq 3.8$, the ground state is a singlet. We find that there are two other values, $J_2\approx 1.9$ and 1.1 , where the nature of the spin correlations changes significantly. Many of the correlations become very small or change sign at those two points. The structure factor seems to indicate crossovers at those points between ground states with different kinds of short-range correlations. In the region $1.1\leq J_2\leq 1.9$, the canted spin configuration in Fig. 1 is consistent with the ED data representing the short-range spin-spin correlations, whereas for larger J_2 up to the ferrimagnetic phase transition point, the commensurate spiral phase with a period of four lattice spacings seems to be in accord to the ED data for $N=12$. It is clear, however, that the periodic boundary conditions imposed on the chain prevent the appearance of the periodic structures with larger periods predicted by the classical analysis.

For $J_2\leq 1$, the correlations between the spin- $\frac{1}{2}$ sites show an unusual pattern, namely, the spin- $\frac{1}{2}$ sites appear to decompose into two sublattices such that each sublattice has a substantial antiferromagnetic coupling within itself (with a strong frustration), but the coupling between the two sublattices is much weaker. We call this system the next-nearest-neighbor antiferromagnet (NNN-AFM). In Sec. IV, we use a

perturbative expansion in J_2 and an effective Hamiltonian description to provide some understanding of why this happens. This seems to be a remarkable property of the spin- $\frac{1}{2}$ -spin-1 sawtooth system.

In Sec. V, we will consider the particular case of $J_2=2$ where we find that the system shows an interesting behavior if a magnetic field is applied with a strength which is close to the saturation value h_s , i.e., the value above which all the spins are aligned with the field. We will show that for $J_2=2$, the system displays a macroscopic jump in the magnetization as the magnetic field crosses h_s . This phenomenon is known to occur in some other strongly frustrated quantum spin systems.¹⁴⁻¹⁶

II. SPIN-WAVE ANALYSIS

To develop the SWT, we assume that the values of the spin S_1 and S_2 are much larger than 1. We will describe how to obtain the spin-wave dispersion up to order S_i . This is called linear SWT because interactions between the spin-waves do not appear at this order. Since some of the classical ground states considered in this section have a coplanar configuration of the spins, it is convenient to use a technique for deriving the spin-wave spectrum which can be applied to both collinear and coplanar configurations. For a coplanar configuration, let us assume that the spins lie in the z - x plane. Consider a particular spin of magnitude S which points at an angle ϕ with respect to the \hat{z} direction. Then we can write the Holstein-Primakoff representation for that spin as

$$\begin{aligned}\cos\phi S_z + \sin\phi S_x &= S - a^\dagger a, \\ -\sin\phi S_z + \cos\phi S_x + iS_y &= \sqrt{2S - a^\dagger a} a, \\ -\sin\phi S_z + \cos\phi S_x - iS_y &= a^\dagger \sqrt{2S - a^\dagger a},\end{aligned}\quad (2)$$

where $[a, a^\dagger]=1$. We now introduce a coordinate and a momentum, $q=(a+a^\dagger)/\sqrt{2}$ and $p=i(a^\dagger-a)/\sqrt{2}$, satisfying $[q, p]=i$. On expanding Eq. (2) up to quadratic order in a and a^\dagger , we obtain

$$\begin{aligned}S_z &= \cos\phi[S + \frac{1}{2} - \frac{1}{2}(p^2 + q^2)] - \sin\phi\sqrt{S}q, \\ S_x &= \sin\phi[S + \frac{1}{2} - \frac{1}{2}(p^2 + q^2)] + \cos\phi\sqrt{S}q, \\ S_y &= \sqrt{S}p.\end{aligned}\quad (3)$$

We now consider a general Heisenberg Hamiltonian of the form

$$H = \sum_{ij} J_{ij} \vec{S}_i \cdot \vec{S}_j, \quad (4)$$

where we count each bond (ij) only once, and the spin at site i will be assumed to have a magnitude S_i . Consider a classical configuration in which the spin at site i lies in the z - x plane at an angle ϕ_i with respect to the \hat{z} axis. The condition for this configuration to be a ground state classically is that

$$E_{cl}(\phi_i) = \sum_{ij} J_{ij} S_i S_j \cos(\phi_i - \phi_j) \quad (5)$$

should be a minimum with respect to each of the angles ϕ_i . We must therefore have

$$\sum_j J_{ij} S_i S_j \sin(\phi_i - \phi_j) = 0 \quad (6)$$

for every value of i . Using Eq. (3) and keeping terms up to order S_i , we find that the spin-wave Hamiltonian is given by

$$\begin{aligned} H_{sw} = & \sum_{ij} J_{ij} \left[\left(S_i S_j + \frac{S_i}{2} + \frac{S_j}{2} \right) \cos(\phi_i - \phi_j) \right. \\ & - \frac{1}{2} \cos(\phi_i - \phi_j) (S_j p_i^2 + S_j q_i^2 + S_i p_j^2 + S_i q_j^2) \\ & \left. + \sqrt{S_i S_j} \cos(\phi_i - \phi_j) q_i q_j + \sqrt{S_i S_j} p_i p_j \right]. \quad (7) \end{aligned}$$

The factor of $S_i S_j + S_i/2 + S_j/2$ in this expression appears on expanding a product such as $(S_i + 1/2)(S_j + 1/2)$ coming from Eq. (4) and dropping the term of order 1.

We can obtain the spin-wave spectrum from Eq. (7) as follows. The unit cell of our system is a triangle containing the two sites with spins S_1 and S_2 which lie on its left edge. Let us label the triangles by n , where $n = 1, 2, \dots, N$, and let $a = 1, 2$ denote the spins S_1 and S_2 , respectively; thus each site is labeled as (a, n) . The mapping from the site labels

used in Fig. 1 to the site labels (a, n) being used here is as follows: $n \rightarrow (2, n)$ if $1 \leq n \leq N$, and $n \rightarrow (1, n - N)$ if $N + 1 \leq n \leq 2N$. We define the Fourier transforms

$$\begin{aligned} p_{a,k} &= \frac{1}{\sqrt{N}} \sum_n p_{a,n} e^{-ikn}, \\ q_{a,k} &= \frac{1}{\sqrt{N}} \sum_n q_{a,n} e^{-ikn}, \end{aligned} \quad (8)$$

where $-\pi < k \leq \pi$. These operators satisfy the commutation relation $[q_{a,k}, p_{b,k'}] = i \delta_{ab} \delta_{k,-k'}$. Let us now assume that the cosines appearing in Eq. (7) take the following simple forms: they are equal to $\cos \alpha$ for every pair of neighboring spin- S_1 sites, and equal to $\cos \beta$ for every pair of neighboring spin- S_1 -spin- S_2 sites. (We will see below that this may happen even in situations where the angles $\phi_{a,n}$ are themselves not the same in all the triangles). Up to terms of order S_i , the Hamiltonian in Eq. (1) takes the form

$$H = E_{0,cl} + \sum_{ab} \sum_k [p_{a,-k} M_{ab,k} p_{b,k} + q_{a,-k} N_{ab,k} q_{b,k}], \quad (9)$$

$$E_{0,cl} = N \left[(S_1^2 + S_1) \cos \alpha + 2J_2 \left(S_1 S_2 + \frac{S_1}{2} + \frac{S_2}{2} \right) \cos \beta \right],$$

where $E_{0,cl}$ is the classical ground-state energy, and

$$\begin{aligned} M_{ab,k} &= \begin{pmatrix} S_1 \cos k - S_1 \cos \alpha - J_2 S_2 \cos \beta & J_2 \sqrt{S_1 S_2} (1 + e^{-ik})/2 \\ J_2 \sqrt{S_1 S_2} (1 + e^{ik})/2 & -J_2 S_1 \cos \beta \end{pmatrix}, \\ N_{ab,k} &= \begin{pmatrix} S_1 \cos \alpha \cos k - S_1 \cos \alpha - J_2 S_2 \cos \beta & J_2 \sqrt{S_1 S_2} \cos \beta (1 + e^{-ik})/2 \\ J_2 \sqrt{S_1 S_2} \cos \beta (1 + e^{ik})/2 & -J_2 S_1 \cos \beta \end{pmatrix}. \end{aligned} \quad (10)$$

Note that the 2×2 matrices M_k and N_k satisfy $M_{-k} = M_k^T$ and $N_{-k} = N_k^T$. If we write $p_{a,k}$ and $q_{a,k}$ as the columns p_k and q_k , respectively, then the classical Hamiltonian equations of motion take the form

$$\frac{dq_k}{dt} = 2M_k p_k \quad \text{and} \quad \frac{dp_k}{dt} = -2N_k q_k. \quad (11)$$

For each value of k , the harmonic solutions of these equations have two possible frequencies ω_k given by the eigenvalue equation

$$\det(4M_k N_k - \omega_k^2 I) = 0. \quad (12)$$

The quantum-mechanical energy levels are then given by $(n_{a,k} + 1/2)\omega_{a,k}$, where $n_{a,k}$ is the occupation number of the mode labeled as (a, k) , where a can take two different values. Note that the frequencies $\omega_{a,k}$ are the same in all the

coplanar configurations. Hence the zero-point energy given by $(1/2)\sum_{a,k}\omega_{a,k}$ does not break the classical degeneracy between the different configurations.

We can now obtain the spin-wave dispersion for various values of J_2 . For large values of J_2 , the classical ground state is a collinear ferrimagnetic configuration in which the S_1 spins point in one direction, say, the \hat{z} direction, and the S_2 spins point in the opposite direction; the total spin of the ground state is therefore equal to $N(S_1 - S_2)$. Hence the cosines in Eq. (10) are given by $\cos \alpha = 1$ and $\cos \beta = -1$. The spin wave dispersions are then given by

$$\omega_{\pm,k} = 2\sqrt{a_k^2 - c_k^2} \pm 2b_k, \quad (13)$$

$$a_k = \frac{J_2}{2}(S_1 + S_2) - S_1 \sin^2\left(\frac{k}{2}\right),$$

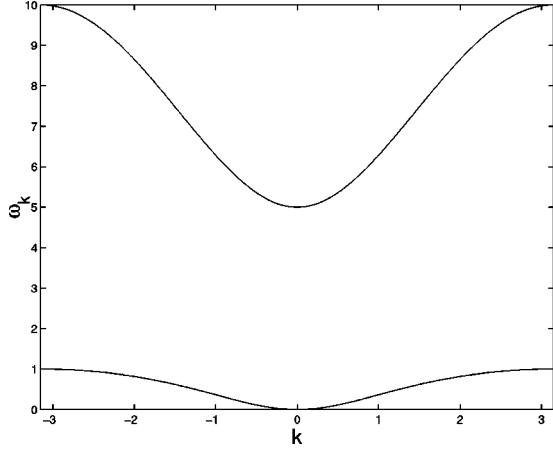


FIG. 2. Spin-wave dispersions in the ferrimagnetic phase for $J_2=5$, $S_1=1$, and $S_2=0.5$.

$$b_k = \frac{J_2}{2}(S_1 - S_2) + S_1 \sin^2\left(\frac{k}{2}\right),$$

$$c_k = J_2 \sqrt{S_1 S_2} \cos\left(\frac{k}{2}\right).$$

[We can show that the upper branch $\omega_{+,k}$ corresponds to excitations with total spin one more than the ground-state spin, while the lower branch $\omega_{-,k}$ corresponds to excitations with total spin one less than the ground-state spin]. These dispersions are shown in Fig. 2 for $J_2=5$, $S_1=1$ and $S_2=0.5$. At $k=0$, we find that $\omega_{+,0}=2J_2(S_1-S_2)$ and $\omega_{-,0}=0$. At $k=\pi$, $\omega_{+,\pi}=2J_2S_1$ while $\omega_{-,\pi}=2J_2S_2-4S_1$. When the ratio J_2 decreases to the value $2S_1/S_2$, the lower branch $\omega_{-,k}$ vanishes for all values of k . This signals an instability to some other state for $J_2 < 2S_1/S_2$.

For later use, we note that up to order S_i , the ground-state energy per unit cell in the ferrimagnetic phase is given by

$$\begin{aligned} \frac{E_0}{N} &= E_{0,cl} + \frac{1}{2} \int_{-\pi}^{\pi} \frac{dk}{2\pi} (\omega_{+,k} + \omega_{-,k}) \\ &= S_1^2 + S_1 - 2J_2 \left(S_1 S_2 + \frac{S_1}{2} + \frac{S_2}{2} \right) + \int_0^{\pi} \frac{dk}{2\pi} 4 \sqrt{a_k^2 - c_k^2}, \end{aligned} \quad (14)$$

where a_k and c_k are given in Eq. (13).

For $J_2 < 2S_1/S_2$, the classical ground state is no longer a collinear state. To see this, note that the Hamiltonian in Eq. (1) can be written, up to a constant, as $H = (1/2) \sum_n \vec{W}_n^2$, where

$$\vec{W}_n = J_2 \vec{S}_{2,n} + \vec{S}_{1,n} + \vec{S}_{1,n+1}. \quad (15)$$

Thus the classical ground state is one in which the vector \vec{W}_n has the minimum possible magnitude in each triangle n . For $J_2 < 2S_1/S_2$, we find that the lowest-energy state in each triangle is one in which the magnitude of \vec{W}_n is zero; this is

given by a configuration in which the spin- S_2 makes an angle of $\pi - \theta$ with both the spin- S_1 's, while the angle between the two spin- S_1 's is 2θ , where

$$\theta = \cos^{-1} \left(\frac{J_2 S_2}{2S_1} \right). \quad (16)$$

Figure 1 shows a particularly simple example of such a configuration in which all the spin- S_2 's are aligned with each other; this is called the canted state. It is clear that there is an infinite number of such configurations even in a system with a finite number of triangles. This is because, in a triangle labeled n , we can continuously rotate the spins $S_{2,n}$ and $S_{1,n+1}$ around the spin $S_{1,n}$ while maintaining the relative angles at the values given above. In many systems with such an enormous ground-state degeneracy, it is known that the zero-point energy in linear SWT breaks the degeneracy partially by selecting only the coplanar ground states; this is called the order-from-disorder phenomenon.¹⁷ Let us therefore consider only coplanar configurations, in which all the spins lie in the z - x plane. Even with this restriction, there are about 2^N different configurations, because in triangle n , there are two possible directions of the spins $S_{2,n}$ and $S_{1,n+1}$ for a given direction of the spin $S_{1,n}$.

Let us compute the spin-wave dispersion in a coplanar configuration. The cosines in Eq. (10) are given by

$$\begin{aligned} \cos \alpha &= \cos(2\theta) = \frac{J_2^2 S_2^2}{2S_1^2} - 1, \\ \cos \beta &= -\cos \theta = -\frac{J_2 S_2}{2S_1}. \end{aligned} \quad (17)$$

We then find that $\det M_k = 0$ for all values of k . Equation (12) then implies that one of the frequencies, say, $\omega_{-,k} = 0$ for all k . We thus have a dispersionless zero mode. This mode arises due to the invariance of the classical ground-state energy under certain kinds of continuous rotations in each triangle as mentioned above. In the problem of the Heisenberg anti-ferromagnet on the kagomé lattice, it is known that interactions between spin waves, which appear when we go to higher orders in the $1/S$ expansion, remove the degeneracy in the zero-mode branch,¹⁸ and produce a low-lying spin wave branch with an energy scale proportional to $S^{2/3}$. We will restrict ourselves to linear SWT here, and will not consider such corrections to the zero-mode branch.

Since $\omega_{-,k} = 0$, the other frequency can be obtained from Eq. (12) as

$$\begin{aligned} \omega_{+,k}^2 &= 4 \operatorname{tr}(M_k N_k) \\ &= 2J_2^2 S_2^2 (\cos k - J_2)(1 + \cos k) + 4S_1^2 \sin^2 k + J_2^4 S_2^2. \end{aligned} \quad (18)$$

This dispersion is shown in Fig. 3 for $J_2=2$, $S_1=1$, and $S_2=0.5$. At $k=\pi$, we have $\omega_{+,\pi} = J_2^2 S_2$, while at $k=0$, we have $\omega_{+,0} = J_2 S_2 |2 - J_2|$. We thus see that the gap vanishes at $k=0$ if $J_2=2$.

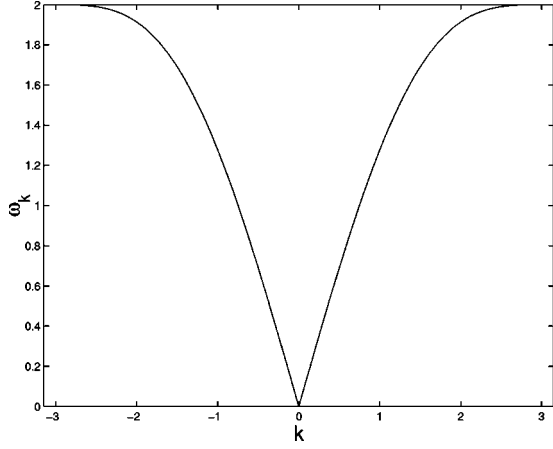


FIG. 3. Nonvanishing spin-wave dispersion in the singlet phase for $J_2=2$, $S_1=1$, and $S_2=0.5$.

Up to order S_i , the ground-state energy per unit cell in the coplanar phase is given by

$$\frac{E_0}{N} = -S_1^2 - S_1 - \frac{J_2^2}{2}(S_2^2 + S_2) + \int_0^\pi \frac{dk}{2\pi} \omega_{+,k}, \quad (19)$$

where $\omega_{+,k}$ is given in Eq. (18). One can check that the expressions (14) and (19) match at $J_2=2S_1/S_2$.

Let us now comment on a special feature of the value $J_2=2$. Within the set of 2^N classical coplanar ground states, the total spin of the system can have a wide range of values depending on the exact configuration of the spins. We can see this by noting that the total spin can be written as $\vec{S}_{tot} = \sum_n \vec{V}_n$, where

$$\vec{V}_n \equiv \vec{S}_{2,n} + \frac{1}{2}(\vec{S}_{1,n} + \vec{S}_{1,n+1}). \quad (20)$$

In any of the classical ground states for $J_2 < 2S_1/S_2$, we find that the magnitude of this vector is given by $|\vec{V}_n| = |S_2 + S_1 \cos \beta| = (S_2/2)|2 - J_2|$. Depending on how the vectors \vec{V}_n in different triangles add up, the total spin of the system can therefore range from 0 to $(NS_2/2)|2 - J_2|$. However, if $J_2=2$, we see that \vec{V}_n is proportional to \vec{W}_n in Eq. (15); hence all the classical ground states have zero spin since we know that each of the vectors \vec{W}_n has zero magnitude. Quantum mechanically, we expect the exponentially large classical degeneracy to be broken by tunneling; however we would still expect an unusually large number of low-energy singlet excitations for $J_2=2$.

Another special value of J_2 is given by $J_2=1$. At this point, the Hamiltonian of a single triangle is given by the square of the total spin $\vec{S}_n = \vec{S}_{2,n} + \vec{S}_{1,n} + \vec{S}_{1,n+1}$. Thus the total spin of each triangle vanishes in any of the classical ground states.

Finally, we can use this formalism to obtain the spin-wave dispersion close to the fully aligned ferromagnetic state which is the ground state when a sufficiently strong magnetic field is applied; this will be useful for the discussion in Sec. V. Let us consider a Hamiltonian which is the sum of the one given in Eq. (1) and a magnetic field term given by

$$H_{mag} = -h \sum_{i=1}^{2N} S_{i,z}, \quad (21)$$

where we have assumed the same value of the gyromagnetic ratio g for spins S_1 and S_2 , and we have absorbed g in the definition of the magnetic field h . If h is large enough, the ground state is one in which the angle ϕ in Eq. (2) is equal to zero for all the spins. Following the procedure described above, we see that the matrices $M_{ab,k}$ and $N_{ab,k}$ are equal to each other and are given by

$$M_{ab,k} = N_{ab,k} = \begin{pmatrix} S_1 \cos k - S_1 - J_2 S_2 + h/2 & J_2 \sqrt{S_1 S_2} (1 + e^{-ik})/2 \\ J_2 \sqrt{S_1 S_2} (1 + e^{ik})/2 & -J_2 S_1 + h/2 \end{pmatrix}. \quad (22)$$

We then find that the spin-wave dispersions are given by

$$\omega_{\pm,k} = h - J_2(S_1 + S_2) - 2S_1 s_k \pm \sqrt{J_2^2(S_1 + S_2)^2 + 4J_2 S_1(S_2 - S_1 - J_2 S_2)s_k + 4S_1^2 s_k^2},$$

$$s_k = \sin^2\left(\frac{k}{2}\right). \quad (23)$$

III. NUMERICAL RESULTS

We have used the Lanczos algorithm to study the ground-state properties of the sawtooth chain with $S_1=1$ and $S_2=1/2$ for even values of N from 4 to 12 with periodic boundary conditions. To reduce the sizes of the Hilbert spaces, we work in subspaces with a given value of the total component of the spin S_z and the momentum, since these operators commute with the Hamiltonian. If $S_z=0$, we reduce the Hilbert space further by working in subspaces in which the spin parity P_s is equal to ± 1 ; under the transformation P_s , the values of S_z at all the sites are flipped from $S_{iz} \rightarrow -S_{iz}$. (P_s transforms the operators $S_{iz} \rightarrow -S_{iz}$ and $S_{ix} \rightarrow -S_{ix}$, leaving S_{iy} invariant. It therefore corresponds to a rotation by π about the \hat{y} axis). One can show that the eigenvalue of P_s is related to the total spin S of the state by

$$P_s = (-1)^{N(S_1 + S_2) - S}. \quad (24)$$

Figure 4 shows the total ground-state energy as a function of J_2 for $N=8$. The solid line shows the numerical data, while the dashed line shows the spin-wave results obtained from Eq. (19) for $J_2 \leq 4$, and from Eq. (14) for $J_2 \geq 4$. We do not present the data for $N=12$ since the latter are almost indistinguishable from those presented in Fig. 4. In the inset, the solid lines show piecewise linear fits to the numerical data to the left and right of $J_2=3.8$, while the dotted lines show the continuations of the same two straight lines to the right and left of $J_2=3.8$, respectively. This shows a small discontinuity in the slope at $J_2 \approx 3.8$; we find that $(1/N)dE_0/dJ_2$ is equal to -1.25 and -1.45 to the left and

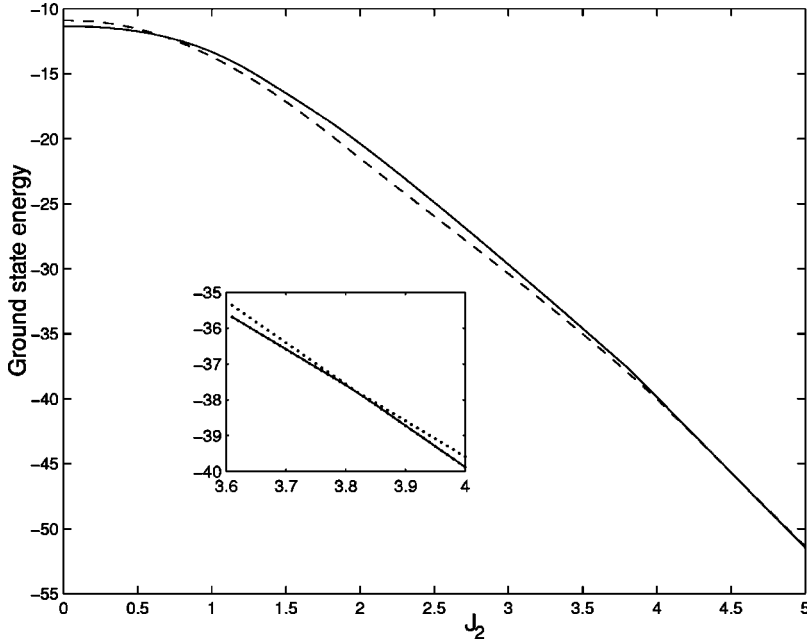


FIG. 4. Total ground-state energy as a function of J_2 . The solid line shows the numerical data from exact diagonalization for a chain with eight triangles, while the dashed line shows the spin wave results. In the inset, the solid lines show piecewise linear fits to the numerical data to the left and right of $J_2=3.8$, while the dotted lines show the continuations of the same two straight lines to the right and left of $J_2=3.8$, respectively. This shows a small discontinuity in the slope at $J_2 \approx 3.8$.

right, respectively, of $J_2 = 3.8$. These numbers agree with the nearest neighbor spin- $\frac{1}{2}$ -spin-1 correlations discussed in Eq. (25) and Fig. 7 below.

For both $N=8$ and $N=12$, we find that the total spin of the ground state changes abruptly at $J_2 \approx 3.8$. For $J_2 \geq 3.8$, the ground state spin has the ferrimagnetic value of $N(S_1 - S_2) = N/2$. For $J_2 \leq 3.8$, the ground state is a singlet. The number 3.8 compares reasonably with the SWT value of $2S_1/S_2 = 4$, considering that SWT is only expected to be

accurate for large values of S_1 and S_2 . The total spin of the first excited state, however, shows a more complicated behavior as J_2 is varied; this is plotted in Fig. 5 for $N=8$. For $J_2 \geq 3.9$, the first excited state has a spin of 3 as expected from the spin-wave calculations. For $J_2 \leq 2.9$, the first excited state is a singlet. For $2.9 \leq J_2 \leq 3.9$, the spin of the first excited state fluctuates considerably. The fluctuations near $J_2 \approx 3.9$ may be due to the finite size of the system, and they may disappear in the thermodynamic limit.

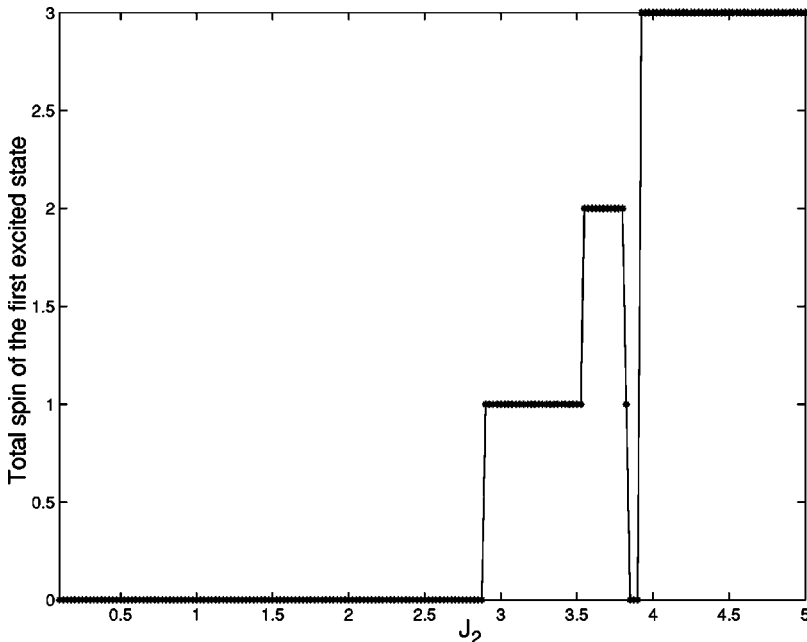


FIG. 5. Total spin of the first excited state as a function of J_2 for a chain with eight triangles.

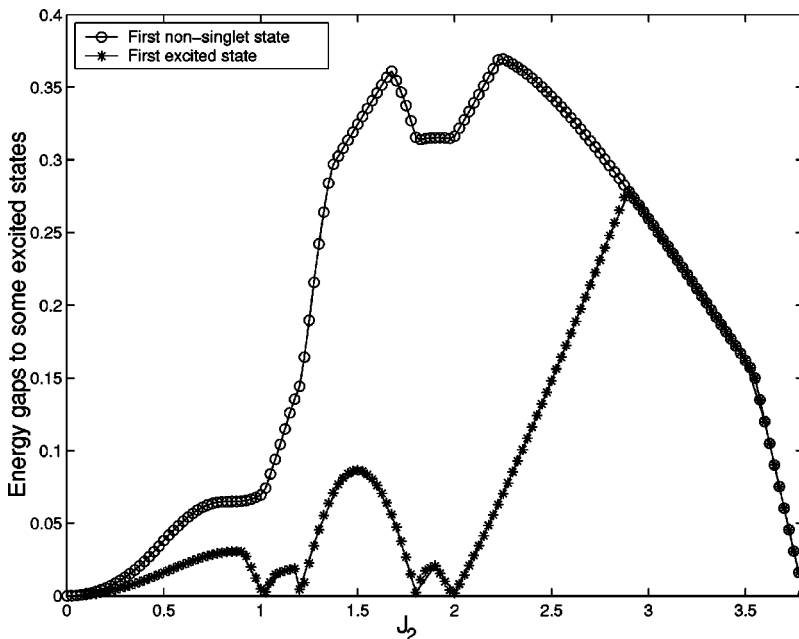


FIG. 6. Energy gaps between the ground state and the first excited state (lower curve) and the first nonsinglet state (upper curve) as a function of J_2 for a chain with 8 triangles. The ground state is a singlet for the range of J_2 shown in the figure. For $J_2 < 2.9$, the first excited state is a singlet, while for $J_2 > 2.9$, the first excited state is the same as the first nonsinglet state.

For $J_2 \leq 3.8$ and $N=8$, the energy gaps between the ground state and the first excited state (whose spin is shown in Fig. 5) and the first nonsinglet state are plotted as functions of J_2 in Fig. 6; the two gaps are shown by stars and circles, respectively. From Fig. 5, we see that the first excited state is a singlet for $J_2 < 2.9$ and is nonsinglet for $J_2 > 2.9$ (except for a few values of J_2 close to 3.9). Hence, the first excited state is the same as the first nonsinglet state for $J_2 > 2.9$ as shown in Fig. 6. Although the gap to the first excited state fluctuates, we see that it is particularly small near $J_2 = 1$ and 2. These small gaps may represent either level crossings of the ground state (as discussed below) or genuine low-lying singlet excitations; it is difficult to distinguish between these two possibilities without going to much larger system sizes. We note that low-lying singlet excitations are known to occur in the spin- $\frac{1}{2}$ Heisenberg antiferromagnet on a kagomé lattice which is a well-known example of a highly frustrated system.¹⁹ For $0.5 \leq J_2 \leq 2.5$, we see that the gap to the first excited state (which is a singlet) is typically much smaller than the gap to the first nonsinglet state. In fact, we find that in this range of J_2 , there are several singlet excitations which lie below the first nonsinglet excitation. For instance, for $N=12$, we find four and eight singlet excitations lying below the first nonsinglet excitation at $J_2=1$ and 2, respectively.

For $N=12$, the ground state has the following properties. For $J_2 \leq 3.85$, the ground state is a singlet, and the parity symmetry in the subspace with $S_z=0$ is given by $P_s=1$. However, the momentum k of the ground state repeatedly changes between 0 and π . This is shown in Table I. We observe that there are several crossings, particularly near $J_2 = 1.1$ and 1.9. Repeated level crossings such as this in a

finite-sized system are often a sign of a spiral phase in the thermodynamic limit;²⁰ we will discuss this possibility in more detail below.

Next, we examine the two-spin correlations $\langle \vec{S}_i \cdot \vec{S}_j \rangle$ in the ground state. These are of three types: spin- $\frac{1}{2}$ -spin-1, spin-1-spin-1, and spin- $\frac{1}{2}$ -spin- $\frac{1}{2}$. These are shown in Figs. 7–9 for $N=12$. We have only shown six correlations in each case. All the other correlations are related to these by translation and reflection symmetries. The behaviors of all the correlations show large changes near three particular values of J_2 , namely, 1.1, 1.9, and 3.8. For instance, many of the correlations approach zero or change sign near these three values.

It is particularly instructive to look at the nearest-neighbor spin- $\frac{1}{2}$ -spin-1 correlation, i.e., $\langle \vec{S}_1 \cdot \vec{S}_{14} \rangle$ in Fig. 7. By the Feynman-Hellmann theorem, this is related to the derivative with respect to J_2 of the ground-state energy per triangle,

$$\frac{1}{N} \frac{dE_0}{dJ_2} = 2 \langle \vec{S}_1 \cdot \vec{S}_{14} \rangle, \quad (25)$$

TABLE I. Ground-state momentum for various values of J_2 , for a chain with 12 triangles.

Range of J_2	Ground-state momentum
$0 < J_2 < 0.95$	π
$0.95 < J_2 < 1.05$	0
$1.05 < J_2 < 1.26$	π
$1.26 < J_2 < 1.78$	0
$1.78 < J_2 < 1.82$	π
$1.82 < J_2 < 1.99$	0
$1.99 < J_2 < 3.75$	π
$3.75 < J_2 < 3.85$	0

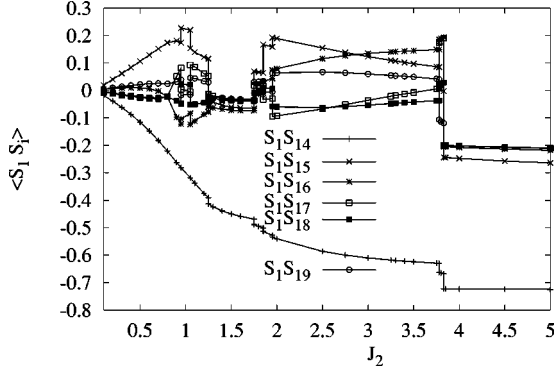


FIG. 7. The spin- $\frac{1}{2}$ -spin-1 correlations as functions of J_2 for a chain with 12 triangles.

where we have used the fact that all the nearest-neighbor spin- $\frac{1}{2}$ -spin-1 correlations are equal. We can see from Fig. 7 that the derivative (25) shows a jump at $J_2 \approx 3.8$, which indicates a first-order transition; we know that the ground-state spin changes abruptly at that point from $N/2$ to 0 without going through any of the intermediate values. The jump in the values of $\langle \vec{S}_1 \cdot \vec{S}_{14} \rangle$ at $J_2 \approx 3.8$ is consistent with the jump in the slope of the ground state energy in Fig. 4 as discussed above. At $J_2 \approx 1.25$ and 1.75 , Eq. (25) seems to show a change of slope but no jump. This could indicate either a second-order transition or a crossover at those points; it is difficult to distinguish between these two possibilities since a change of slope can also arise due to finite-size effects.

For small values of J_2 , we observe that the spin-1-spin-1 correlations in Fig. 8 decay rapidly with the separation n between the two sites, and they also oscillate as $(-1)^n$. This is expected for small J_2 because the spin-1 chain is only weakly coupled to the spin- $\frac{1}{2}$'s; a pure spin-1 antiferromagnetic chain exhibits a Haldane gap and a finite correlation length of about six lattice spacings.^{21,22} The weak coupling also explains why the spin- $\frac{1}{2}$ -spin-1 correlations in Fig. 7 are small. However, the spin- $\frac{1}{2}$ -spin- $\frac{1}{2}$ correlations in Fig. 9 show an unexpected behavior for small J_2 . We find that the spin- $\frac{1}{2}$'s on even and odd sites appear to decouple into two separate chains, with the correlation being very small between spins belonging to different chains; within each chain, the correlations have an antiferromagnetic character. In other words, $\langle \vec{S}_{2i} \cdot \vec{S}_{2j} \rangle$ is small if $i-j$ is odd, and it oscillates as $(-1)^{(i-j)/2}$ if $i-j$ is even. We call this the NNN-AFM. In the following section, we will provide some understanding of this behavior.

To understand better the nature of the changes in the ground state, we looked at the structure factors for the spin-1-spin-1 and spin- $\frac{1}{2}$ -spin- $\frac{1}{2}$ correlations. These are respectively defined as

$$S^{11}(q) = \frac{1}{N} \sum_{i=1}^N \langle \vec{S}_{N+1} \cdot \vec{S}_{N+i} \rangle \cos(qr_i),$$

$$S^{22}(q) = \frac{4}{N} \sum_{i=1}^N \langle \vec{S}_1 \cdot \vec{S}_i \rangle \cos(qr_i), \quad (26)$$

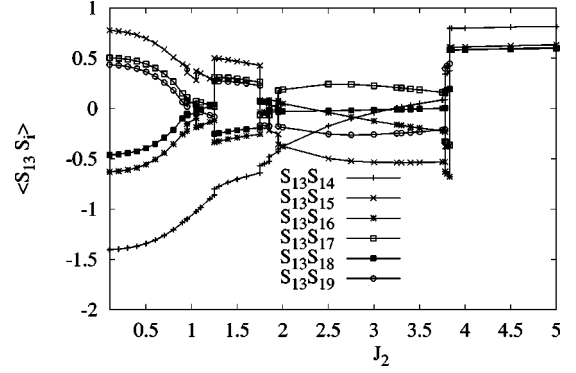


FIG. 8. The spin-1-spin-1 correlations as functions of J_2 for a chain with 12 triangles.

where we define

$$r_i = i - 1 \quad \text{for} \quad 1 \leq i \leq \frac{N}{2},$$

$$= N + 1 - i \quad \text{for} \quad \frac{N}{2} + 1 \leq i \leq N, \quad (27)$$

to account for the periodic boundary conditions, and q takes the values $2\pi n/N$, where $n=0,1,\dots,N-1$. We have included the factors of $1/S_i^2$ (equal to 1 and 4 for spin-1 and spin- $\frac{1}{2}$, respectively) on the right-hand sides of Eq. (26) to make it easier to compare the magnitudes of $S^{11}(q)$ and $S^{22}(q)$.

In Fig. 10, we show the values of q where the two structure factors are maximum (q_{max}) as a function of J_2 for $N=12$. For $0 < J_2 \leq 1$, $q_{max} = \pi/2$ for spin- $\frac{1}{2}$ and π for spin-1. The NNN-AFM behavior of the spin- $\frac{1}{2}$'s discussed in the following section will explain why $q_{max} = \pi/2$ for spin- $\frac{1}{2}$ for small values of J_2 . For $1.25 \leq J_2 \leq 1.75$, $q_{max} = 0$ for spin- $\frac{1}{2}$ and π for spin-1; this suggests that the ground state is in a canted state with a period of two unit cells as shown in Fig. 1. For $1.9 \leq J_2 \leq 3.8$, $q_{max} = \pi/2$ for both spin- $\frac{1}{2}$ and spin-1; this suggests a spiral phase with a period of four unit cells. Finally, for $J_2 \geq 3.8$, q_{max} is equal to 0 for both spin- $\frac{1}{2}$ and spin-1; this is expected in the ferrimagnetic state.

It is possible that the period two and period four states which are suggested by the structure factor for $N=12$ (the

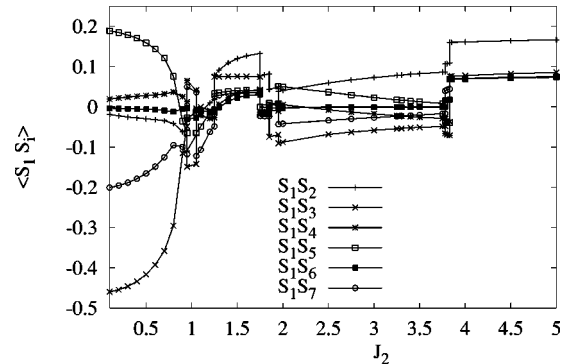


FIG. 9. The spin- $\frac{1}{2}$ -spin- $\frac{1}{2}$ correlations as functions of J_2 for a chain with 12 triangles.

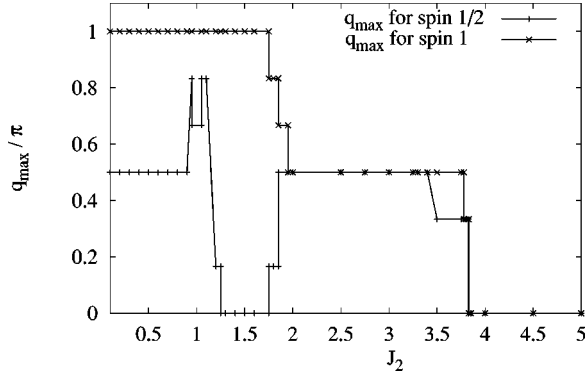


FIG. 10. Values of q where the structure factors $S^{11}(q)$ and $S^{22}(q)$ are maximum as functions of J_2 for a chain with 12 triangles.

periodic boundary conditions only allow some limited periodicities for small systems) will turn into states with longer periods (which change more smoothly with J_2) if we go to larger system sizes. The repeated level crossings between $k=0$ and π shown in Table I also support this scenario.²⁰

Figure 11 shows the values of $S^{ii}(q_{max})$ as a function of J_2 . Once again, we see large fluctuations near $J_2=1.1$, 1.9 , and 3.8 . The structure factors are relatively large for both large (ferrimagnetic) and small values of J_2 , and is smaller for intermediate values of J_2 .

Finally, we examined the possibility of dimerization, namely, whether the ground state spontaneously breaks the invariance of the Hamiltonian under translation by one unit cell. The unit cell of our system has half-odd-integer spin, and such systems are quite susceptible to dimerization in one dimension. A simple way to study this question is to see if the difference between the spin- $\frac{1}{2}$ -spin- $\frac{1}{2}$ correlations between site 1 and its neighbors at sites 2 and N , i.e., $d = \langle \vec{S}_1 \cdot \vec{S}_2 \rangle - \langle \vec{S}_1 \cdot \vec{S}_N \rangle$, is not equal to zero. The problem is that the energy eigenstates we have found are also eigenstates of momentum and are therefore translation invariant; hence the dimerization order parameter d will vanish in such states. A finite system cannot spontaneously break a symmetry such as translation invariance. However, if dimerization does occur, we expect that the ground state (called $|1\rangle$) will be almost degenerate with an excited state (called $|2\rangle$);²³ we

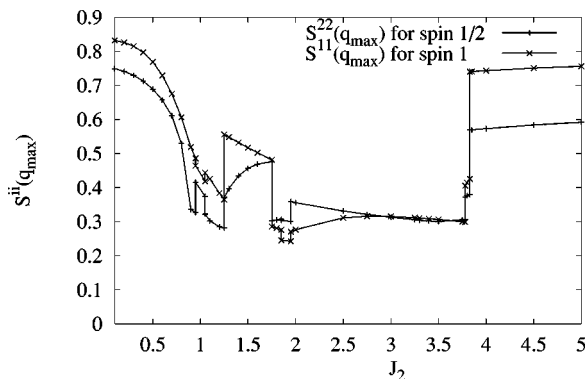


FIG. 11. The structure factors $S^{11}(q_{max})$ and $S^{22}(q_{max})$ as functions of J_2 for a chain with 12 triangles.

TABLE II. The correlations of a spin- $\frac{1}{2}$ with its two neighboring spin- $\frac{1}{2}$'s in the ground state ($|1\rangle$), first excited state ($|2\rangle$), and the two linear combinations ($|2+\rangle$ and $|2-\rangle$) at $J_2=1$ and 2 , for $N=8$.

J_2	State	$\langle \vec{S}_1 \cdot \vec{S}_2 \rangle$	$\langle \vec{S}_1 \cdot \vec{S}_8 \rangle$
1	$ 1\rangle$	-0.00562	-0.00561
1	$ 2\rangle$	-0.07239	-0.07240
1	$ 2+\rangle$	-0.15152	0.07350
1	$ 2-\rangle$	0.07351	-0.15151
2	$ 1\rangle$	0.04198	0.04195
2	$ 2\rangle$	0.06867	0.06871
2	$ 2+\rangle$	0.09063	0.02004
2	$ 2-\rangle$	0.02002	0.09062

can think of these two states as arising from tunneling between the two dimerized states which would be eigenstates of the Hamiltonian for the infinite system. Although the states $|1\rangle$ and $|2\rangle$ would be eigenstates of momentum and therefore translation invariant, the linear combinations $|2+\rangle = (|1\rangle + |2\rangle)/\sqrt{2}$ and $|2-\rangle = (|1\rangle - |2\rangle)/\sqrt{2}$ would not be translation invariant, and may therefore exhibit different values of the parameter d . We are motivated here by the Majumdar-Ghosh model; this is a Heisenberg antiferromagnetic spin- $\frac{1}{2}$ chain in which the next-nearest-neighbor coupling has half the value of the nearest-neighbor coupling.²⁴ This model is known to have two degenerate ground states given by the direct products

$$|\Psi_+\rangle = \prod_{n \text{ odd}} |\psi_{n,n+1}\rangle \quad \text{and} \quad |\Psi_-\rangle = \prod_{n \text{ even}} |\psi_{n,n+1}\rangle, \quad (8)$$

where $|\psi_{n,n+1}\rangle \equiv (|\uparrow_n \downarrow_{n+1}\rangle - |\downarrow_n \uparrow_{n+1}\rangle)/\sqrt{2}$. We observe that $|\Psi_+\rangle$ and $|\Psi_-\rangle$ show dimerization (namely, the parameter d takes the values $\pm 3/4$), but are not invariant under translation by one site. On the other hand, the linear combinations $|\Psi_1\rangle = |\Psi_+\rangle + |\Psi_-\rangle$ and $|\Psi_2\rangle = |\Psi_+\rangle - |\Psi_-\rangle$ do not show dimerization, but are translation invariant.

Returning to our system, we see from Fig. 6 that the ground state is almost degenerate with the first excited state (and both are singlets) at two values of J_2 , namely, 1 and 2. We therefore examine the two correlations mentioned above in the four states $|1\rangle$, $|2\rangle$, $|2+\rangle$, and $|2-\rangle$ at those two values of J_2 . The results are shown in Table II. We see that the states $|2+\rangle$ and $|2-\rangle$ do show an asymmetry in the two nearest-neighbor correlations, and the values of the correlations are exchanged between the two states. However, the numerical values of all the correlations are quite small, so there is no clear evidence for dimerization.

IV. NEXT-NEAREST-NEIGHBOR ANTIFERROMAGNET NEAR $J_2=0$

In this section, we will study the system for small values of J_2 using perturbation theory and the idea of an effective Hamiltonian. A more detailed discussion of the ideas in this section is given in Ref. 25. We write the Hamiltonian in Eq.

(1) as the sum $H=H_0+V$, where

$$H_0 = \sum_{i=N+1}^{2N} \vec{S}_i \cdot \vec{S}_{i+1},$$

$$V = J_2 \sum_{i=1}^N \vec{S}_i \cdot (\vec{S}_{i+N} + \vec{S}_{i+N+1}). \quad (29)$$

For $J_2=0$, we have an antiferromagnetic spin-1 chain with a coupling equal to 1, and N decoupled spin- $\frac{1}{2}$'s. Every state of the system will have a degeneracy of 2^N due to the decoupled spin- $\frac{1}{2}$'s. It is known that the ground state of a spin-1 chain is a singlet with an energy $E_0^1 = -1.40148N$, and it is separated by a gap of $\Delta E^1 = 0.41050$ from the first excited state which is a triplet.²²

Let us denote the eigenstates of H_0 for the spin-1 chain by $|\psi_i^1\rangle$ with energy E_i^1 , where $i=0$ denotes the ground state. The states of the spin- $\frac{1}{2}$ sites will be denoted by $|\psi_j^{1/2}\rangle$. The eigenstates of the full Hamiltonian H can therefore be written as linear combinations of the form

$$|\psi_a\rangle = \sum_{i,j} c_{a,i,j} |\psi_i^1\rangle \otimes |\psi_j^{1/2}\rangle, \quad (30)$$

where the $c_{a,i,j}$ are appropriate coefficients.

We will now expand up to second order in the perturbation V to find an effective Hamiltonian H_{eff} which acts within the subspace of the 2^N ground states which are degenerate for $J_2=0$. The Hamiltonian H_{eff} will only act on the spin- $\frac{1}{2}$'s. To first order in V , we have $H_{1,eff} = \langle \psi_0^1 | V | \psi_0^1 \rangle$. Since V involves both spin- $\frac{1}{2}$ and spin-1 operators, and the expectation value in $H_{1,eff}$ is being taken in a spin-1 state, $H_{1,eff}$ will only involve spin- $\frac{1}{2}$ operators as desired. Now, the expectation value in $H_{1,eff}$ is equal to zero, because V is linear in the spin-1 operators (which are not rotationally invariant), while $|\psi_0^1\rangle$ is a singlet and is therefore rotationally invariant.

We therefore have to go to second order in V . We then have

$$H_{2,eff} = \sum_{i \neq 0} \frac{\langle \psi_0^1 | V | \psi_i^1 \rangle \langle \psi_i^1 | V | \psi_0^1 \rangle}{E_0^1 - E_i^1}, \quad (31)$$

Clearly, this will be an operator which is of degree 2 or less in the spin- $\frac{1}{2}$ operators. Since the state $|\psi_0^1\rangle$, the sum over states $\sum_{i \neq 0} |\psi_i^1\rangle \langle \psi_i^1| / (E_0^1 - E_i^1)$ and V are all invariant under rotations and translations, $H_{2,eff}$ must have the same invariances. The only operators which are of degree 2 or less in spin- $\frac{1}{2}$'s and are rotationally invariant are a constant and products of the form $\vec{S}_i \cdot \vec{S}_j$. Using translation invariance, we see that $H_{2,eff}$ must take the form

$$H_{2,eff} = Na + NJ_2^2 b + J_2^2 \sum_i (c_1 \vec{S}_i \cdot \vec{S}_{i+1} + c_2 \vec{S}_i \cdot \vec{S}_{i+2} + c_3 \vec{S}_i \cdot \vec{S}_{i+3} + \dots) \quad (32)$$

where a, b, c_1, c_2, \dots are numbers which are independent of J_2 , and appropriate periodic boundary conditions are as-

sumed in the summations over i . For a periodic system with N spin- $\frac{1}{2}$'s, the subscript i of c_i goes from 1 to $N/2$ (since N is even), so a total of $2+N/2$ numbers have to be determined. These numbers will depend on the system size; however, since the ground state of a spin-1 chain has a finite correlation length, we would expect these numbers to converge quickly to some values as N becomes large. (We will assume that J_2 is small enough so that terms of order J_2^3 and higher can be neglected in comparison with the terms of order J_2^2 which we are interested in).

A direct computation of the constants a, b, c_i in Eq. (32) using the expression in Eq. (31) is difficult because we would need to accurately determine all the energy levels and eigenstates of a spin-1 chain as well as all the matrix elements appearing in that expression. We therefore assume the form in Eq. (32) (which we have so far found purely on grounds of symmetry), and numerically determine the constants as follows. To determine the first number a in Eq. (32), we set $J_2=0$ and numerically find the ground-state energy which is equal to Na . Next, we turn on the J_2 couplings on the bonds connecting only two of the spin- $\frac{1}{2}$'s, say at sites 1 and $n+1$, to the spin-1's. In other words, we set four of the spin- $\frac{1}{2}$ -spin-1 couplings equal to J_2 , and keep all the other spin- $\frac{1}{2}$ -spin-1 couplings equal to zero; let us call this truncated perturbation $V_1 + V_{n+1}$ (thus, $V = \sum_i V_i$). We ignore the $N-2$ spin- $\frac{1}{2}$'s which are not coupled to the spin-1's. The energy levels of the system consisting of the spin-1 chain and two spin- $\frac{1}{2}$'s will have four low-lying states which would be degenerate with an energy of Na if all the J_2 's had been set equal to zero. These four states are described by an effective Hamiltonian involving the two spin- $\frac{1}{2}$'s of the form

$$H_{i,j,eff} = Na + J_2^2 (2b + c_n \vec{S}_1 \cdot \vec{S}_{n+1}). \quad (33)$$

The important point is that the constants b and c_n in this expression have the same values as in Eq. (32) where all the J_2 couplings are turned on. The reason for this can be traced back to the expression in Eq. (31) which can be used for either the full perturbation V or the truncated perturbation $V_1 + V_{n+1}$. A comparison between the two second-order expressions shows that the constant b arises from the product of a spin- $\frac{1}{2}$ operator at site 1 with itself when we take the product of the two matrix elements in Eq. (31); that is why it appears with a factor of N in Eq. (32) and a factor of 2 in Eq. (33). On the other hand, the constant c_n comes from a product of a spin- $\frac{1}{2}$ operator at site 1 with a spin- $\frac{1}{2}$ operator at site $n+1$, and it comes with the same factor in Eqs. (32) and (33).

We can numerically determine the constants b and c_n from the energies of the four low-lying states of the spin-1 chain plus two spin- $\frac{1}{2}$'s; three of these states will form a triplet with the same energy and one will form a singlet, so that there will be only two equations in two unknowns. We can then repeat the procedure and determine all the constants c_i by successively coupling various pairs of spin- $\frac{1}{2}$'s to the spin-1 chain; in each case, we only have to look at the four low-lying energy levels to find b and c_i . (The values of b that we get in the different cases should of course agree with each other). This procedure will work provided that J_2 is

small enough that the four-low lying energy levels lie far below the gap ΔE^1 of the pure spin-1 chain, and the terms of third and higher orders are much smaller than those of second order. On the other hand, if we choose J_2 to be too small, the energy splittings of J_2^2 are very small, and the determination of the constants b and c_i will suffer from large numerical uncertainties. For our calculations with $N=8$, we found that taking $J_2=0.1$ gives reasonably accurate and self-consistent results. We found the following values of the six numbers:

$$\begin{aligned} a &= -1.417\,12, & b &= -0.126\,65, \\ c_1 &= 0.0183, & c_2 &= 0.1291, \\ c_3 &= -0.0108, & c_4 &= 0.0942. \end{aligned} \quad (34)$$

We see that the value of a found for $N=8$ agrees quite well with the thermodynamic value ($N \rightarrow \infty$) of $-1.401\,48$ quoted earlier.²²

Looking at the values of c_i in Eq. (34), we observe the curious pattern that c_2 is the largest number, followed by c_4 ; the numbers c_1 and c_3 are much smaller in comparison. Thus the spin- $\frac{1}{2}$'s governed by the effective Hamiltonian in Eq. (32) seem to break up into two chains, one consisting of the odd numbered sites, and the other with the even numbered sites. Each of the chains has a nearest-neighbor coupling of $c_2 J_2^2$ which is antiferromagnetic; we therefore call this the NNN-AFM. This explains the numerical result that the structure factor of the spin- $\frac{1}{2}$'s is peaked at $q = \pi/2$ and that the next-nearest-neighbor correlation is the largest in magnitude (and has a negative sign) for small J_2 .

Note, however, that the next-nearest-neighbor coupling in each chain (proportional to c_4 which is about 0.73 times c_2) is also antiferromagnetic and is not much smaller than the nearest-neighbor coupling, so each of the spin- $\frac{1}{2}$ chains is strongly frustrated. For such a strong frustration, it is known that a spin- $\frac{1}{2}$ chain is disordered with a small correlation length of about two lattice spacings (this implies a correlation length of about four lattice spacings in the sawtooth system), and is also strongly dimerized.²⁶ The small correlation length is supported by the correlation data for $N=12$ and $J_2=0.1$; we find that the ratio of spin- $\frac{1}{2}$ -spin- $\frac{1}{2}$ correlations $\langle \vec{S}_1 \cdot \vec{S}_5 \rangle / \langle \vec{S}_1 \cdot \vec{S}_3 \rangle \approx -0.411$, while the ratio of spin-1-spin-1 correlations $\langle \vec{S}_{13} \cdot \vec{S}_{15} \rangle / \langle \vec{S}_{13} \cdot \vec{S}_{14} \rangle \approx -0.552$. Thus the spin- $\frac{1}{2}$ correlations (within each chain) decay faster with increasing distance than the spin-1 correlations (which have a correlation length of six lattice spacings).

To examine the possibility of dimerization, we use a method similar to the one used at the end of Sec. III to look for dimerization at $J_2=1$ and 2. However, the present case is different for the following reasons. First, we are now considering a NNN-AFM, so we have to check if the spin- $\frac{1}{2}$ -spin- $\frac{1}{2}$ correlations between a site and its next-nearest-neighbors are equal. Secondly, we have to simultaneously look for dimerization in the two spin- $\frac{1}{2}$ chains which are almost decoupled from each other. If there is dimerization, we expect four low-lying states which are almost degenerate with each other. For $N=8$, these four states will exhibit dimerization in the four

TABLE III. The correlations of the spin- $\frac{1}{2}$'s at sites 1 and 2 with their two next-nearest-neighboring spin- $\frac{1}{2}$'s in the ground state ($|1\rangle$), first excited states ($|2\rangle$ and $|3\rangle$), and the four linear combinations ($|2\pm\rangle$ and $|3\pm\rangle$) at $J_2=0.1$, for $N=8$.

State	$\langle \vec{S}_1 \cdot \vec{S}_3 \rangle$	$\langle \vec{S}_1 \cdot \vec{S}_7 \rangle$	$\langle \vec{S}_2 \cdot \vec{S}_4 \rangle$	$\langle \vec{S}_2 \cdot \vec{S}_8 \rangle$
$ 1\rangle$	-0.497 65	-0.497 65	-0.497 65	-0.497 65
$ 2\rangle$	-0.246 30	-0.246 29	-0.246 30	-0.246 31
$ 3\rangle$	-0.246 39	-0.246 38	-0.246 25	-0.246 24
$ 2+\rangle$	-0.067 74	-0.676 20	-0.676 20	-0.067 75
$ 2-\rangle$	-0.676 21	-0.067 74	-0.067 75	-0.676 21
$ 3+\rangle$	-0.067 81	-0.676 22	-0.067 65	-0.676 24
$ 3-\rangle$	-0.676 23	-0.067 81	-0.676 25	-0.067 65

quantities $\langle \vec{S}_1 \cdot \vec{S}_3 \rangle$, $\langle \vec{S}_1 \cdot \vec{S}_7 \rangle$, $\langle \vec{S}_2 \cdot \vec{S}_4 \rangle$, and $\langle \vec{S}_2 \cdot \vec{S}_8 \rangle$. For $J_2 = 0.1$, we find that there is a nondegenerate ground state $|1\rangle$, and two degenerate excited states ($|2\rangle$ and $|3\rangle$) which are separated from the ground state by a small gap of 0.000 674. (The next excited state, $|4\rangle$, is separated from the ground state by a gap of 0.001 277; for simplicity, we will not include this state in the following computations). The states $|1\rangle$, $|2\rangle$, and $|3\rangle$ are all translation invariant, and therefore cannot show dimerization. We therefore consider the four linear combinations, $|2\pm\rangle = (|1\rangle \pm |2\rangle) / \sqrt{2}$ and $|3\pm\rangle = (|1\rangle \pm |3\rangle) / \sqrt{2}$ which are not translation invariant. We then compute the four correlations mentioned above in all the seven states; the results are shown in Table III. We observe a substantial amount of dimerization in the states $|2\pm\rangle$ and $|3\pm\rangle$. If we define the dimerization in the two chains to be²⁶

$$\begin{aligned} d_1 &= \langle \vec{S}_1 \cdot \vec{S}_3 \rangle - \langle \vec{S}_1 \cdot \vec{S}_7 \rangle, \\ d_2 &= \langle \vec{S}_2 \cdot \vec{S}_4 \rangle - \langle \vec{S}_2 \cdot \vec{S}_8 \rangle, \end{aligned} \quad (35)$$

we see that the dimerizations in states $|2\pm\rangle$ and $|3\pm\rangle$ are both equal to about ± 0.6085 . Further, the correlations in these four states show all the four possible patterns of dimerization which can occur for two chains.

The occurrence of a NNN-AFM with strong frustration for small values of J_2 is one of the interesting features of the spin- $\frac{1}{2}$ -spin-1 sawtooth chain. Although the spin-1 chain is gapped and therefore plays no direct role at energy scales much smaller than $J_1=1$, it perturbatively induces an unusual kind of interaction between the spin- $\frac{1}{2}$'s which leads to a nontrivial behavior for that subsystem.

V. MACROSCOPIC MAGNETIZATION JUMP AT $J_2=2$

In this section, we will discuss the phenomenon of a macroscopic magnetization jump which occurs in the sawtooth chain for arbitrary values of S_1 and S_2 if $J_2=2$. In general, this phenomenon can occur in highly frustrated quantum antiferromagnets in which one of the spin wave modes (above the fully polarized ferromagnetic state) is completely dispersionless. When a uniform magnetic field is applied to the system, the magnetization can show a macroscopic jump at the saturation field h_s (defined as the minimum field for

which all the spins are aligned in the ground state).¹⁴⁻¹⁶ By macroscopic we mean that the magnetization per unit cell jumps by a finite amount Δm at $h=h_s$. This occurs if (i) there is a special kind of ferromagnetic one-magnon eigenstate of the Hamiltonian which is spatially localized (a few lattice spacings), (ii) this eigenstate has the lowest energy amongst all the one-magnon eigenstates, (iii) the energy of this one-magnon state is negative with respect to the fully aligned state if $h < h_s$, and (iv) there are no multimagnon bound states with energy lower than the sum of the individual one-magnon states. If all these conditions are satisfied, then for a certain range of values of the magnetic field below h_s , the lowest energy state is one in which there is a macroscopic number of these magnons localized in disjoint regions of the lattice. Eventually, as the field h is increased, the energy of these magnons will cross zero at $h=h_s$ and then turn positive; for $h > h_s$, therefore, the lowest energy state will be the one in which all the spins are aligned with the field. Hence there will be a macroscopic magnetization jump at h_s .

For the sawtooth chain with spins S_1 and S_2 , we consider a Hamiltonian which is the sum of the ones given in Eqs. (1) and (21). The spin wave dispersion in this case is given in Eq. (23). For $J_2=2$, we see that the one-magnon states (above the fully aligned state) have two branches with the dispersions $\omega_- = h - 4(S_1 + S_2)$ (which is independent of the momentum and is equal to the energy of the localized one-magnon state $|\psi_n\rangle$ discussed below), and $\omega_+ = h - 4S_1 \sin^2(k/2)$ which is greater than ω_- for all values of k . On the other hand, the special one-magnon state (above the fully aligned state) is a superposition of three states: $|2, n-1\rangle$ in which the spin- S_2 in triangle $n-1$ has $S_z = S_2 - 1$ (and all the other spins have the maximum possible values of S_z), $|1, n\rangle$ in which the spin- S_1 in triangle n has $S_z = S_1 - 1$, and $|2, n\rangle$ in which the spin- S_2 in triangle n has $S_z = S_2 - 1$. The particular superposition of these three states which is an eigenstate of the total Hamiltonian is given by

$$|\psi_n\rangle = |2, n-1\rangle + |2, n\rangle - 2\sqrt{\frac{S_2}{S_1}}|1, n\rangle. \quad (36)$$

The energy of this state with respect to the fully aligned state is given by $E = h - 4(S_1 + S_2)$. The total spin of this state is $N(S_1 + S_2) - 1$, since it has total $S_z = N(S_1 + S_2) - 1$ and is annihilated by total S_+ . We thus see that the special one-magnon state has the lowest energy amongst all the one-magnon eigenstates.

We thus see that the state $|\psi_n\rangle$ meets the conditions (i) and (ii) given above, and its energy is lower than that of the fully aligned state if $h < h_s$, where

$$h_s = 4(S_1 + S_2). \quad (37)$$

We therefore identify h_s as the saturation field, and we expect a macroscopic jump in the magnetization when h crosses h_s . The magnitude of the magnetization jump can be found as follows. Since each of the special one-magnon states involves three sites, at most $N/2$ such states can exist

in disconnected regions of a chain with N triangles. The lowest energy of a state with n magnons will be less than the energy of the fully aligned state by an amount equal to $n[h - 4(S_1 + S_2)]$ as long as $n \leq N/2$. Once the number of magnons exceeds $N/2$, some of them will be close enough to interact (repulsively) with each other, and we no longer expect the energy to vary linearly with the number of magnons. Hence, when the magnetic field is lowered slightly below h_s , we expect the magnetization to abruptly drop from the maximum possible value of $M_{max} = N(S_1 + S_2)$ to $M_{max} - N/2$. The magnetization jump is therefore given by $\Delta M = N/2$. The ratio $\Delta M / M_{max} = 1/2(S_1 + S_2)$ goes to zero in the classical limit $S_1, S_2 \rightarrow \infty$. The magnetization jump is therefore a true quantum effect as emphasized in Ref. 14.

For general values of S_1 and S_2 , we have not analytically checked condition (iv) that there are no multimagnon bound states with energy lower than the sum of one-magnon bound states. However, this is numerically found to be true in many models due to the absence of attractive interactions between the magnons.¹⁴⁻¹⁶ This is also found to be true in our system with $S_1 = 1$ and $S_2 = 1/2$, as the data given below shows.

For $N = 12$, we numerically find that in the absence of a magnetic field, the lowest energy E_0 in subspaces with different values of the total S_z is given by, $E_0(S_z = 18) = 36$, $E_0(S_z = 17) = 30$, $E_0(S_z = 16) = 24, \dots$, $E_0(S_z = 12) = 0$, and $E_0(S_z = 11) = -5.167392$. Thus, when the magnetic field strength is lowered just below $h_s = 6$, the magnetization jumps abruptly from 18 to 12 in accordance with the arguments given above. We would like to note here that since the one-magnon state in Eq. (36) is strongly localized, the phenomenon of macroscopic magnetization jump (in particular, the value of h_s) is free of finite-size effects.

VI. DISCUSSION

We have studied the ground-state and low-energy properties of a spin- $\frac{1}{2}$ -spin-1 sawtooth chain using SWT and exact diagonalization of finite systems. Linear SWT shows that there are two phases, the ground state being ferrimagnetic in one phase and a singlet in the other phase, separated by the value of $J_2 = 4$. In addition, $J_2 = 2$ is special because all the classically degenerate states have total spin equal to zero at that point, and $J_1 = 1$ is special because the total spin in each triangle is zero in all the classical ground states.

Numerically, we have studied the model for only three values of N , namely, 4, 8, and 12, for the following reasons. The next-nearest-neighbor antiferromagnetic behavior discussed in Sec. IV implies that the spin- $\frac{1}{2}$ subsystem would be frustrated by the periodic boundary conditions for odd values of $N/2$; hence, numerical results for small values of N such as 6 and 10 would not provide an accurate guide to the properties of the model in the thermodynamic limit. Hence, we have restricted ourselves to even values of $N/2$. The next possible value of $N = 16$ is beyond our existing computational resources.

Our numerical studies indicate that there are four distinct regions. For $J_2 \geq 3.8$, the ground state is ferrimagnetic, while for $J_2 \leq 3.8$, it is a singlet. The structure factors suggest that the ground state is in a short ranged spiral state with a period

of four unit cells for $1.9 \leq J_2 \leq 3.8$, and in a short ranged canted state with a period of two unit cells for $1.1 \leq J_2 \leq 3.8$. Near $J_2 = 1$ and 2, the gap between the ground state and the first excited state is particularly small, and there are repeated level crossings, possibly indicating crossovers between ground states with different kinds of short-range correlations. Numerical calculations on larger system sizes would be very useful for a complete understanding of the nature of the ground state for $1 \leq J_2 \leq 3.8$. Finally, the spin- $\frac{1}{2}$'s form an interesting system called a NNN-AFM for J_2

≤ 1 ; the ground state of this system has a short correlation length and is strongly dimerized.

ACKNOWLEDGMENTS

D.S. acknowledges the Department of Science and Technology, India for financial support through Grant No. SP/S2/M-11/00. N.B.I. and J.R. acknowledge the Deutsche Forschungsgemeinschaft for financial support (Projects Nos. 436BUL/17/5/03 and Ri 615/6-1). J.R. is indebted to J. Schulenburg for numerical assistance.

*Permanent address: Institute of Solid State Physics, Bulgarian Academy of Sciences, Tsarigradsko chausse 72, 1784 Sofia, Bulgaria.

¹C. Lhuillier and G. Misguich, in *High magnetic fields*, edited by C. Berthier, L.P. Lévy and G. Martinez (Springer-Verlag, Berlin, 2001), Vol. 595, pp. 161–190.

²T. Nakamura and K. Kubo, Phys. Rev. B **53**, 6393 (1996); K. Kubo, *ibid.* **48**, 10 552 (1993).

³D. Sen, B.S. Shastry, R.E. Walstedt, and R. Cava, Phys. Rev. B **53**, 6401 (1996).

⁴S.A. Blundell and M.D. Nunez-Reguerio, Eur. Phys. J. B **31**, 453 (2003).

⁵C. Raghunathan, I. Rudra, S. Ramasesha, and D. Sen, Phys. Rev. B **62**, 9484 (2000).

⁶N.B. Ivanov, J. Richter, and U. Schollwöck, Phys. Rev. B **58**, 14 456 (1998); J. Richter, U. Schollwöck, and N.B. Ivanov, Physica B **281&282**, 845 (2000); N.B. Ivanov and U. Schollwöck, in *Some Contemporary Problems of Condensed Matter Physics*, edited by V.V. Dvoeglazov (Nova Science Publishers, New York, 2001).

⁷P. Azaria, C. Hooley, P. Lecheminant, C. Lhuillier, and A.M. Tsvelik, Phys. Rev. Lett. **81**, 1694 (1998); S.K. Pati and R.R.P. Singh, Phys. Rev. B **60**, 7695 (1999).

⁸Ch. Waldtmann, H. Kreutzmann, U. Schollwöck, K. Maisinger, and H.-U. Everts, Phys. Rev. B **62**, 9472 (2000).

⁹S.K. Pati, Phys. Rev. B **67**, 184411 (2003).

¹⁰N. Maeshima, M. Hagiwara, Y. Narumi, K. Kindo, T.C. Kobayashi, and K. Okunishi, Scr. Mater. **15**, 3607 (2003).

¹¹P. Fulde, A.N. Yaresko, A.A. Zvyagin, and Y. Grin, Europhys. Lett. **54**, 779 (2001).

¹²S. Sachdev, *Quantum Phase Transitions* (Cambridge University Press, Cambridge, 1999).

¹³P.W. Anderson, Physica A **86**, 694 (1952); R. Kubo, *ibid.* **87**, 568 (1952).

¹⁴J. Schulenburg, A. Honecker, J. Schnack, J. Richter, and H.-J. Schmidt, Phys. Rev. Lett. **88**, 167207 (2002).

¹⁵J. Schnack, H.-J. Schmidt, J. Richter, and J. Schulenburg, Eur. Phys. J. B **24**, 475 (2001).

¹⁶J. Richter, J. Schulenburg, A. Honecker, J. Schnack, and H.-J. Schmidt, J. Phys. Condens. Matter **16**, S779 (2004).

¹⁷B. Douçot and P. Simon, J. Phys. A **31**, 5855 (1998).

¹⁸A. Chubukov, Phys. Rev. Lett. **69**, 832 (1992).

¹⁹P. Lecheminant, B. Bernu, C. Lhuillier, L. Pierre, and P. Sindzingre, Phys. Rev. B **56**, 2521 (1997); Ch. Waldtmann, H.-U. Everts, B. Bernu, P. Sindzingre, C. Lhuillier, P. Lecheminant, and L. Pierre, Eur. Phys. J. B **2**, 501 (1998).

²⁰T. Tonegawa and I. Harada, J. Phys. Soc. Jpn. **56**, 2153 (1987); **58**, 2902 (1989).

²¹F.D.M. Haldane, Phys. Lett. **93A**, 464 (1983); Phys. Rev. Lett. **50**, 1153 (1983).

²²S.R. White and D.A. Huse, Phys. Rev. B **48**, 3844 (1993).

²³M. Oshikawa, M. Yamanaka, and I. Affleck, Phys. Rev. Lett. **78**, 1984 (1997).

²⁴C.K. Majumdar and D.K. Ghosh, J. Math. Phys. **10**, 1388 (1969); **10**, 1399 (1969).

²⁵V. Ravi Chandra, cond-mat/0311560 (unpublished).

²⁶S.R. White and I. Affleck, Phys. Rev. B **54**, 9862 (1996).